Models of nuclear coupling in a circular extra space

Hans-Dieter Herrmann

October 29, 2026

Contents

1 Introduction **2**

2 Models of attractive and repulsive forces **3**
2.1 Dress - coupling and skeleton - coupling 3
2.1.1 The role of fluctuating charge pairs 3
2.1.2 The role of the budget of charge clusters 3
2.2 Contact coupling and Yukawas 'carrier particle' 4
2.3 The coupling of rotons by radial or axial approach 4

3 Deuteron and alpha - particle **7**
3.1 The model of the deuteron 7
3.2 The model of the alpha particle 10

4 Bosonic dineutrons, diprotons and (np) - pairs **15**
4.1 Comparison of the separation energies of dineutron and diproton 15
4.1.1 The internal compensation of attraction and repulsion within a (2n2p) - group 17
4.2 Several dineutrons attached to a nucleus 17
4.3 The local contact points 22
4.4 The binding capacity of a dineutron, a diproton and an (np) - pair 24

5 Nuclear eigenspaces **25**
5.1 The geometry of nuclear eigenspaces of even - even nuclei with Z < 50 25
5.2 The structure of heavy even - even nuclei with Z > 50 31

6 Conclusions **36**

7 Appendix **37**
7.1 Energy factors of circulating charges as function of $z = \alpha/\pi$ . . . 37
7.2 Models of free and bound nucleons 37

Abstract

Mass and magnetic moment of the deuteron, the masses of the alpha-particle and of other light nuclei are reproduced by two types of interaction between models of proton and neutron in its eigenspaces. First the loss of fluctuating charge pairs and second the reduction of the number of charge clusters per mass quantum. The models of proton and neutron used in the article are described in 'Baryon models in a circular extra space', see https://philarchive.org/rec/HERBMI-2 and https://tonsa.de. The first type of interaction represents a new fundamental force, independent of the strong coupling within a single nucleon. The second effect generates identical main structures ('skeleton' masses) of proton and neutron models bound in a nucleus. This guarantees probably the stability of the neutron within the deuteron, the alpha-particle and other nuclei, in contrast to the instability of the free neutron. Both effects cause the binding energy of even – even nuclei. The parameters of interactions of proton and neutron models in 'basic space' (common eigenspaces) replace within the proposed model the self-consistent mean field method of Interacting Boson Models (IBM) in spacetime.

1 Introduction

Nuclear physics describes nuclei with a spherical shape, oblate or prolate deformations, rotations and vibrations, as well as mass and binding energy of the nuclei. The liquid drop model [8], the nuclear shell model [7], cluster model [5], [6], and interacting boson model [9], [10], [16] are successful steps to a theory of nuclear structure.

The article uses a 'dual space concept'. The dual space models of particles and of nuclei consist of two parts.

The first part is the conventional theory in space-time, using e.g. the Hamiltonians of the interacting boson model, an algebraic theory. The second part is the description of nuclei in a circular space, called "basic space". Nuclear theory in basic space considers the internal structure of protons and neutrons, whose constituents circulate with the velocity of light, described in [13].

This article is focused on the second part of the dual space - model.

The huge number of interactions in heavy nuclei makes it necessary to reduce the number of components and also the number of possible interactions. The exact nuclear shell model would lead to intractable computations. Therefore, pairs or larger groups of nucleons are put together to achieve bosonic constituents which do not underlie the Pauli exclusion principle. The number of possible interactions can be reduced by formulation of a self-constent field (in spacetime, see [15]) and by limitation of the number of interaction partners of a bound nucleon (in the eigenspace of a nucleus).

The purpose of this article is to test the basic space models of proton and neutron in order to understand the nuclear coupling. Two topics are of interest: First the development of the nuclear structure from the material structures of

protons and neutrons, and second the formation of the nuclear eigenspace from the eigenspaces of isolated nucleons.

We avoid the combination of rotations in basic space with rotations in space - time. This restriction seems to be justified in the current non-established state of the model. Therefore we don't consider nuclei with spin - orbit couplings. The total spin of an even - even nucleus consisting of bosonic constituents is always zero, we consider only nuclei with the signature $J^P = 0^+$ (total spin zero, positive parity).

The light even - even nuclei with N = Z consist exclusively of (2n2p) - groups. Such a group has the composition of an alpha-particle. However, a (2n2p) - group does not necessarily exist as a 'preformed' alpha - particle in a nucleus, it is normally in a nonlocal mode but entangled concerning the spin - directions. In basic space, this difference between local and non-local mode can be ignored. Thus we consider (2n2p) - groups as the main bosonic constituents of the model of a nucleus, besides the bosonic dineutrons and diprotons.

2 Models of attractive and repulsive forces

2.1 Dress - coupling and skeleton - coupling

2.1.1 The role of fluctuating charge pairs

The baryon models developed in a previous article [13] are desribed in Figs. 40 and 41 in the appendix. The models allow the formation of a common eigenspace of two or three nucleons by radial or axial approach of the dresses of the nucleons. A common eigenspace needs less fluctuating charge pairs and therefore less energy than the eigenspaces of unbound separate nucleons. Thus the loss of fluctuating charge pairs represents the main source of the binding energy of the developing nucleus. The loss of fluctuating charge pairs appears as the main mechanism which causes the attracting nuclear force.

2.1.2 The role of the budget of charge clusters

The number of charge clusters per mass quantum may change during the nuclear coupling. One parton of the neutron, the so called 'light arm' (LA), has in the *free* neutron enhanced mass quanta of the type

$m_4 = w_4^4 m_Q = 3.\,376\,6\ \ MeV$. Each mass quantum is enhanced by the cluster factor $w_4^4 = 1.\,038\,045$.

In the model of the *bound* neutron the LA parton has only half that number of charge clusters and becomes more similar to the proton model. The average cluster factor becomes $\frac{1}{2}(w_4^4+1) = 1.\,019\,022$ and leads to enhanced mass quanta with the average mass

$m_{41} = (\frac{1}{2}w_4^4 + \frac{1}{2})m_Q = 3.\,314\,726\ \ MeV$.

The small mass decrease between m_4 and m_{41} contributes to the binding energy of the neutron in the corresponing bound state like in the deuteron or

in an alpha-particle. The reduction of the budget of charge clusters in the *light block* of the neutron represents a second source of attractive nuclear forces.

The mass quanta of the *heavy blocks* of proton and neutron amount to $m_8 = w_8^8 m_Q = 3.779\,494\ MeV$ in all cases and do not change during the coupling process.

The skeleton of a bound neutron is absolutely identically with the skeleton of a proton. This is possibly the reason for the stability of the bound neutron in contrast to the unstable free neutron.

2.2 Contact coupling and Yukawas 'carrier particle'

Yukawa invented 1934 a theory of the coupling between nucleons by the exchange of a virtual particle [1], [2]. Using the Heisenberg uncertainty relations, Yukawa postulated a mass of this "carrier-particle" of about 100 MeV and a range of about 1 fm ($10^{-15}m$). The muon, discovered 1936 by Anderson and Neddermeyer, was thought to be the Yukawa particle. However, during the next decade it became clear, that the muon is a lepton and has nothing to do with the nuclear force. The discovery of the pion 1947 in cosmic radiation provided an appropriate Yukawa particle, and the meson exchange theory is up to now a successful tool.

The basic space models of proton and neutron (Figs. 40 and 41) have light arms as partons of lowest mass, approximately 107 MeV, very close to the muon mass. The radius of the light arms amounts to 0.92 fm. Thus the lightest birotons of the nucleon models are similar to the Yukawa particle. They do not interact by exchange, however by contact and by sharing fluctuating charge pairs with the contact partner. Their radius is the range of the nuclear attraction. The interaction in long distances could be described by a 'one-pion exchange', the interaction in medium distances by a 'two-pion exchange', using the terminology of Yukawa. This corresponds in the basic space model to the average radii of arms (long distance) and legs (medium distance). The radius definition in basic space takes the role of the Heisenberg uncertainty relation in the Yukawa theory. The virtual character of the Yukawa particle is replaced by the existence of the partons (birotons, nuclear constituents) in basic space. The similarity ends with the repulsion between nucleons at very short distances: The hard core of nucleons could not be described by Yukawas 'pion-exchange' model.

2.3 The coupling of rotons by radial or axial approach

The loss of fluctuating charge pairs during the formation of a common eigenspace represents a special type of the nuclear coupling, the coupling *between* different nucleons. The nuclear force cannot be understood as a 'residuum' of the strong force, the coupling between the partons *within* a nucleon. This assumption extends the number of fundamental forces.

Two rotons belonging to different nucleons need to have parallel spin axes in order to get coupled. Two different geometries of coupling are possible:

- Radial coupling of spin-antiparallel rotons. The spin axes are parallel, however they have always a distance of the order of the two radii of the rotons. The coupled nucleons exist in the same layer. Axial couplig represents the main coupling method.

- Axial coupling of spin-parallel rotons. The spin axes become identically. The coupled nucleons exist in different layers. Axial coupling represents a rare coupling method.

In both cases, the rotons generate a common circular eigenspace with a reduced number of fluctuating charge pairs. The common eigenspace is two-dimensional perpendicular to the spin axis.

The reduction of the number of fluctuating charge pairs reduces the total rotating energy of the coupled system, the difference appears as binding energy of the system.

A mechanical picture could help to illustrate the radial "contact coupling". The tangential movements near the contact site of the spin-antiparallel rotons are identical, both rotons have the same circular velocity of light, +c or -c. The mechanical analogue is a cog wheel. This is schematically drawn in Fig.1.

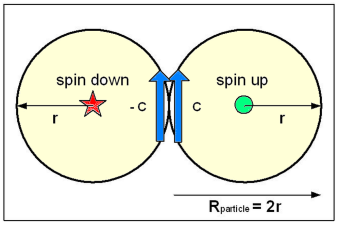


Figure 1: Coupling between *antiparallel* rotons generates attraction caused by radial approach. In contrast, *spin-parallel* rotons have opposite tangential momenta at radial approach, they are 'dense' and inpenetrable for each other in the case of radial approach.

An unlimited approach of the coupled nucleons does not occur because each nucleon consists of six birotons and many rotons have parallel spins, that prevents a collapse of the coupled system by unlimited attraction of the coupled rotons.

The two neighbors of each nucleon in a closed chain of four nucleons generate an attracting force. Antiparallel rotating neighbors could be the origin of the binding within the alpha-particle (see Fig. 2).

The geometry requires a synchronization of the coupled rotons. A synchronous movement could be reached by equal masses of the rotons, leading to equal radii.

The interaction between charged partons within a common eigenspace of bound nucleons comprises the classical p - p - repulsion and several non-classical variants such as p - n - attraction and n - n - repulsion, see Fig. 3.

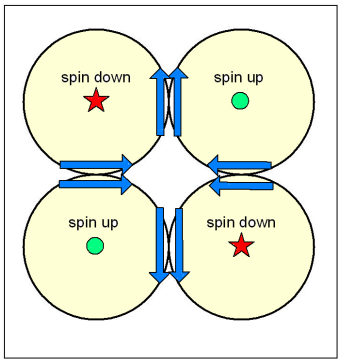


Figure 2: Rotons of four nucleons bound in an alpha-particle in attractive contact-interaction with two antiparallel coupling partners per nucleon. The coupling in the alpha-particle generates a ring-like chain of attraction.

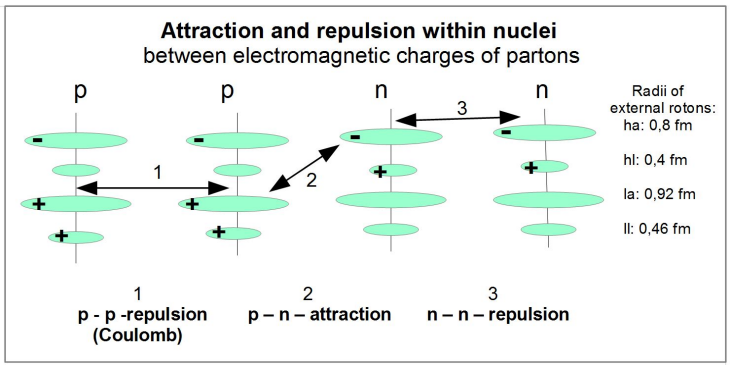


Figure 3: Types of electromagnetic interaction between protons and neutrons. The p - p - interaction is dominated by repulsion, known from classical Coulomb - interaction. The n -p - attraction and the n - n - repulsion are non-classical interaction types. The actual total (np) - interaction is a mix of different types, which can compensate each other.

These different types of interaction occur in combination. Therefore, we try to separate a certain type of interaction whenever possible.

In a first step the deuteron will be discussed as the only stable nucleus consisting of only two nucleons.

3 Deuteron and alpha - particle

3.1 The model of the deuteron

The deuteron $d = (n \uparrow p \uparrow)$ represents the only stable nucleus consisting of only two nucleons. The binding of two spin-parallel nucleons requires a model with binding contact between partons of neutron and proton, where roton one of the neutron interacts with roton two of the proton or vice versa. By this way, a binding between rotons with anti-parallel spins is possible.

The mass of the deuteron $m_d = 1875.61294257(57)\ MeV$ is observed somewhat smaller than the sum of the masses of the free nucleons [1]):

$m_n + m_p = 1877.\,837\,508\,7\ MeV$. The difference is the binding energy B_d of the deuteron:

$B_d = m_n + m_p - m_d = 2.\,224\,566\,11(84)\ MeV$.

The relative anomalous magnetic moment of the deuteron $\mu_d/\mu_N = 0,8574382338(22)$ is observed somewhat smaller than the sum of the relative anomalous magnetic moments of the free nucleons:

$\mu_n/\mu_N + \mu_p/\mu_N = 0.879\,804\,644\,6$, the small decrease is the result of the nuclear binding between neutron and proton:

$\mu_d/\mu_N - (\mu_n/\mu_N + \mu_p/\mu_N) = -0.022\,366\,410$.

The partons called 'heavy arm' (HA) of the models of the free neutron and proton have very similar relative anomalous moments, with the small difference (see Figs. 40 and 41 in the appendix):

$\mu_n/\mu_N(HA) - \mu_p/\mu_N(HA) = -3.\,812\,635\,9 - (-3.\,790\,438\,18) = -0.022\,19\,8$

This difference is near to the difference observed at the parameters of the deuteron. If the two heavy arms of neutron and proton would synchronize caused by their binding, both of its relative magnetic moments would become identically. This would approximately explain the small decrease of the relative anomalous moment of the deuteron. Synchronization of two rotons means identity of the cycle times, achieved by identical rotating masses.

Actually, we assume a change of masses of both heavy arms, which perfectly reproduces the full difference of its relative magnetic moments, it becomes

$\mu_{d,\mathrm{mod}}/\mu_N - (\mu_n/\mu_N + \mu_p/\mu_N) = -0.022\,359\,6$, the absolute deviation from the experimental value amounts to $6.\,8 \times 10^{-6}$.

The higher mass of the HA in the proton decreases remarkably due to the loss of 10 fluctuating charges:

[1] The experimental values for deuteron and alpha-particel are taken from [14].

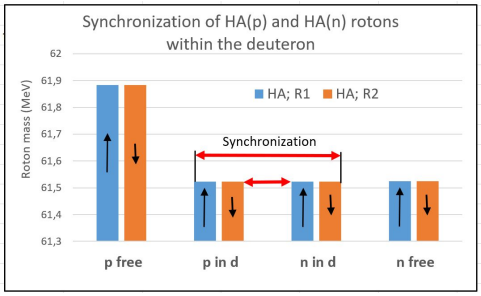


Figure 4: Two spinparallel partons of proton and neutron synchronize within the deuteron.

$123.768\,288 - 123.045\,079\,33 = 0.723\,21\ MeV$, whereas the parton mass in the neutron remains nearly unchanged:

$123.047\,690 - 123.045\,079\,33 = 2.610\,7 \times 10^{-3}\ MeV$

The synchronization of the interacting rotons is illustrated in Fig. 4, the formulas for the calculation of masses and relative magnetic moments of the bound neutron and proton are given in the Figs. 42 and 43 in the appendix.

Two partons of proton and neutron synchronize within the deuteron. The arrows show the spin direction. The 'heavy arm' (HA) of the proton loses mass by the disappearance of 10 fluctuating charges. The reduction of mass causes an increase of the negative relative magnetic moment. This change explains the slight difference between the moment of the deuteron and the sum of the moments of the free p and n.

The masses of the HA partons of the bound proton and neutron become identically, this reduces the deuteron mass by

$123.768\,288 + 123.047\,690 - 2 * 123.045\,079\ = 0.725\,819\ MeV$

This loss of mass contributes to the binding energy of the deuteron.

Another contribution comes from the partial synchronization of the partons 'light arm' (LA) of the nucleons.

The mass of the LA parton of the neutron changes from

$m(LA, n\ free) = (32+28(b_4-1)+(w_8^2+u_{16}-2))m_4 = 108.928\,825\ MeV$ to the value

$m(LA, n\ in\ d) = (32+16(b_4^2-1)+12(b_4-1)+(w_8^2+u_{16}-2))m_{41} == 107.430\,033\ MeV$

The mass of the corresponding parton LA of the proton does not change, but one of its rotons can now be synchronized with one roton of the neutron - LA, see Fig. 5.

The loss of mass of the neutron-LA amounts to

$108.928\,825 - 107.430\,033 = 1.498\,8\ MeV.$

The total mass of neutron and proton decreases due to the binding of the partons HA and LA providing a model value of the binding energy of the deuteron:

$B_{d,\mathrm{mod}} = 0.725\,819 + 1.498\,8 = 2.224\,6\ MeV$, the absolute deviation from the experiment amounts to

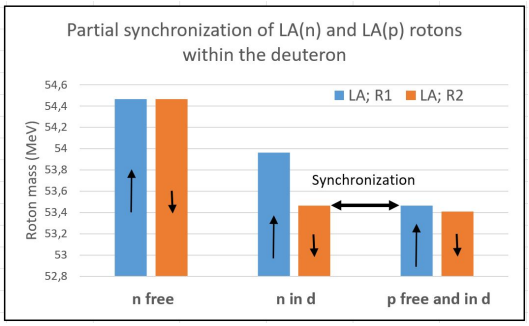


Figure 5: The partial synchronization of two partons of proton and neutron within the deuteron. The arrows show the spin direction of a roton.

n free	N_f	skeleton
H ⊖ ⊕	162	$160m_8$
L	96	$32m_4 + 64m_{41}$
$n \equiv n^0$	258	$256m_Q$

n in d	N_f	skeleton
H ⊖ ⊕	162	$160m_8$
L	102	$96m_{41}$
$n \equiv n^0$	264	$256m_Q$

p free	N_f	skeleton
H ⊖	174	$160m_8$
L ⊕ ⊕	92	$96m_{41}$
$p \equiv p^+$	266	$256m_Q$

p in d	N_f	skeleton
H ⊖	170	$160m_8$
L ⊕ ⊕	88	$96m_{41}$
$p \equiv p^+$	258	$256m_Q$

Figure 6: Changes of the models of p and n due to the binding in a deuteron. The skeleton of the neutron becomes identically to the skeleton of the proton during coupling in the deuteron. The nunber of fluctuating charges N_f changes.

$B_d - B_{d,\mathrm{mod}} = 2.224\,566 - 2.224\,6 = -3.4 \times 10^{-5}\ MeV$.

We remark, that the partial synchronization of the LA partons is connected with a change of the neutron skeleton: It becomes completely identically with the proton skeleton. The enhanced mass quanta

$m_4 = w_4^4 m_Q = 3.376\,602\,5\ MeV$ in the free neutron are replaced by the somewhat lighter mass quanta

$m_{41} = \frac{1}{2}(w_4^4 + 1)m_Q = 3.314\,725\,7\ MeV$ in the bound neutron. This can be interpreted as the reason for the stability of the neutron within the deuteron, whereas the free neutron is unstable.

Fig. 6 gives an overview on the structural changes in the models of proton and neutron during the binding in the deuteron. This table shows the characteristics of the nuclear binding with *one binding partner* of a nucleon.

The complete structure of proton and neutron, bound in a deuteron, is given in the appendix (see Figs. 42 and 43).

The model mass of the deuteron can be summarized as

$$m(np)_1 = (35b_8^2 + 262b_8 + 6w_8 + w_{16}^2 + 6w_{16} + 4u_{32} + 6)m_8 + \quad (1)$$

$$+ (45b_4^2 + 100b_4 + 2w_8^2 + 4u_{16} + 4w_4 + 4w_8 + 33)m_{41} \quad (2)$$

$$= 1875.612\,886\ MeV \quad (3)$$

This result has a relative deviation of $3 * 10^{-8}$ from the experimental value $m_{d,\mathrm{exp}} = 1875.612\ 942\ 57\ MeV$.

The series expansion in fourth order of $z = \alpha/\pi$ provides a relative deviation of $1.6 * 10^{-6}$ from the experimental value.

$$m_{d,\mathrm{mod}} \approx 256 m_Q (2 + \frac{3187}{32} z + \frac{58\,321}{16} z^2 + 102\,852 z^3 + 2416\,509 z^4) \quad (4)$$

$$= 1875.609\,990\ MeV \quad (5)$$

The comparison with the corresponding values of free nucleons gives

$$m_{n,\mathrm{mod}} + m_{p,\mathrm{mod}} \approx 256 m_Q (2 + \frac{3221}{32} z + \frac{58\,881}{16} z^2 + 103\,945 z^3 + 2446\,849 z^4) \quad (6)$$

$$= 1877.834\,559\ MeV \quad (7)$$

The difference yields the binding energy of the deuteron

$$B_{d,\mathrm{mod}} \approx 256 m_Q (\frac{17}{16} z + 35 z^2 + 1093 z^3 + 30\,340 z^4) = 2.224\,569\ \ MeV \quad (8)$$

with a relative deviation of $1.5 * 10^{-6}$ from the observed value $B_{d,\mathrm{exp}} = 2.224\,566\ MeV$.

The series expansions demonstrate, that mass and binding energy of the deuteron depend on two fundamental constants only: The mass quantum m_Q and the finestructure constant α.

The deuteron shows a binding of a nucleon with *one partner - nucleon,* having parallel spins of both nucleons. In contrast, the binding within an alpha particle represents a binding of each nucleon with *two binding partners* having antiparallel spins. This type of nuclear coupling will be discussed in the next section.

3.2 The model of the alpha particle

The extraordinary stability of the alpha-particle $\alpha = (n \uparrow n \downarrow p \uparrow p \downarrow)$ is caused by the full synchronization of all partons of protons and neutrons within the alpha-particle. The partons called 'ears' (E1 and E2) as well as the heavy arms (HA) loose about one half of its fluctuating charges and become identically in neutron and proton, see Fig. 7

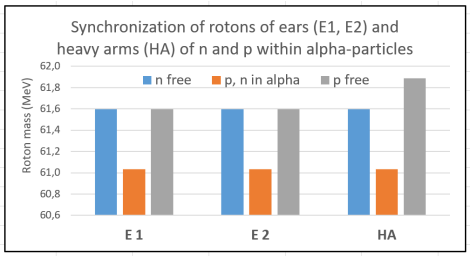


Figure 7: The synchronization of three partons of neutron and proton within an (np) pair of the alpha-particle.Two pairs of coupled rotons of p and n with opposite spins are combined in one orange column.

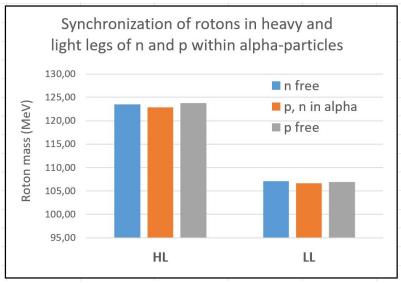


Figure 8: The synchronization of two partons of proton and neutron within a (np)-pair of the alpha-particle..Two pairs of coupled rotons of p and n with opposite spins are combined in one orange column

The synchronization creates common eigenspaces of three partons of neutron and proton within an alpha-particle.

Two pairs of coupled rotons with opposite spins of the partons 'heavy leg' (HL) and 'light leg' (LL) of p and n are combined and shown in one orange column of Fig. 8. However, also after synchronization the HL of the neutrons retain the electroweak charges from the free neutrons and the HL of the protons remain weakly charged only. The light legs of the protons retain their electroweak charges, and so on.

The synchronization of the light arms occurs in the same manner, the LA partons of the protons retain the electroweak charges, see Fig. 9.

The complete formulas for the masses of partons of neutrons and protons within the alpha-particle are given in Figs. 44 and 45 in the appendix.

Fig. 10 contains an overview on the structural changes in the models of proton and neutron during the binding in an alpha-particle. This table shows the characteristics of the nuclear binding with *two binding partners* of a nucleon. N_f means the number of fluctuating charges, given for the heavy block H and the light block L of neutron and proton.

The complete structure of proton and neutron, bound in an alpha-particle,

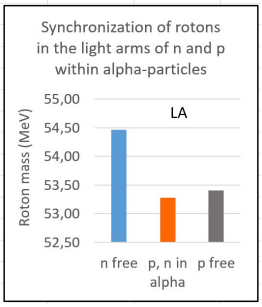


Figure 9: The synchronization of one parton of n and p within a (np)-pair of the alpha-particle. The parton 'light arm' (LA) of the neutron loses more mass during the coupling due to a change in the mass of the skeleton.

n free	N_f	skeleton
H ⊖ ⊕	162	$160m_8$
L	96	$32m_4 + 64m_{41}$
$n \equiv n^0$	258	$256m_Q$

n in α	N_f	skeleton
H ⊖ ⊕	104	$160m_8$
L	48	$96m_{41}$
$n \equiv n^0$	152	$256m_Q$

p free	N_f	skeleton
H ⊖	174	$160m_8$
L ⊕ ⊕	92	$96m_{41}$
$p \equiv p^+$	266	$256m_Q$

p in α	N_f	skeleton
H ⊖	104	$160m_8$
L ⊕ ⊕	44	$96m_{41}$
$p \equiv p^+$	148	$256m_Q$

Figure 10: Changes of the models of p and n due to the binding in the alpha-particle. The skeleton of the neutron becomes identically to the skeleton of the proton during coupling in the alpha-particle.. The nunber of fluctuating charges N_f changes due to thecoupling.

is given in the appendix (see Figs. 44 and 45).

The high degree of synchronization of the neutron and proton models in an alpha particle can be demonstrated by comparison of the masses. One obtains the following masses of a nucleon in an alpha-particle:

$$m_{n,\alpha} = 931.\,852\,648\ MeV \tag{9}$$

$$m_{p,\alpha} = 931.\,837\,125\ MeV \tag{10}$$

The sum defines the mass of a spincompensated (np) pair, bound in an alpha-particle:

$$m(np)_2 = m_{n,\alpha} + m_{p,\alpha} = 1863.\,689\,773\ MeV \tag{11}$$

The model mass of an alpha-particle amounts to

$m_{\alpha,\mathrm{mod}} = 2m(np)_2 = 3727.\,379\,546\ MeV$, compared to the measured value $m_{\alpha,\mathrm{exp}} = 3727.\,379\,411\ MeV$, a relative deviation of $3.6 * 10^{-8}$.

The binding energy of a (np) - pair within an alpha-particle equals

$$B(np)_2 = m_n + m_p - m(np)_2 = 14.147832\ MeV \tag{12}$$

The series expansion of $m(np)_2$ in fourth order of $z = \alpha/\pi$ reads

$$m(np)_2 \approx 256 m_Q (2 + \frac{753}{8} z + \frac{13\,479}{4} z^2 + 93\,136 z^3 + 2156\,416 z^4) \tag{13}$$

$$= 1863.\,687\,218\ MeV \tag{14}$$

Using the comparison to the masses of free nucleons, see equation 6, we obtain an approximation to the binding energy of the alpha-particle:

$$B_{\alpha,\mathrm{mod}} = 2(m_{n,\mathrm{mod}} + m_{p,\mathrm{mod}}) - 2m(np)_2 \tag{15}$$

$$\approx 2 * 256 m_Q (\frac{209}{32} z + \frac{4965}{16} z^2 + 10\,809 z^3 + 290\,433 z^4) \tag{16}$$

$$= 28.\,294\,683\ MeV \tag{17}$$

with a relative deviation of $3.3 * 10^{-5}$ from the observed value $B_{\alpha,\mathrm{exp}} = 28.\,295\,605\,6\ MeV$.

Estimation of the size of an alpha - particle The six partons of a nucleon are birotons, each biroton has a spin of $\frac{1}{4}\hbar$. A biroton consists of an external and an internal roton with the spins $+\frac{1}{2}\hbar,\ -\frac{1}{4}\hbar$. The rotons 1 (external) and 2 (internal) have the radius

$$|\overrightarrow{r_1}| = \frac{\hbar}{2M_1 c}; \quad |\overrightarrow{r_2}| = \frac{\hbar}{4M_2 c} \tag{18}$$

where M_i represents the mass of the $i-$th roton in basic space (the eigenspace of the particle, see [13], Table 1). The roton masses in basic space are twice the masses in space-time, $M_i = 2m_i$. Thus we get the radii of the rotons in the form

$$|\overrightarrow{r_1}| = \frac{\hbar c}{4m_1c^2} \approx \frac{\hbar c}{2m_{pt}c^2}; \quad |\overrightarrow{r_2}| = \frac{\hbar c}{8m_2c^2} \approx \frac{\hbar c}{4m_{pt}c^2} \tag{19}$$

where $m_{pt} \approx m_1 + m_2$ means the mass of one of the six partons of a nucleon. The radii can be obtained in fm from the energy equivalents $m_{pt}c^2$ (MeV) of the particle masses, and using the factor

$\hbar c = 197.\ 326\ 980\ 4\ MeV * fm$

We ask the question, whether the radii, defined in basic space, have a plausible relation to the radii measured in space-time. We assume a quadratic geometry of the eigenspace of an alpha-particle (see Fig. 23), such that two nucleons in radial approach determine the size of the particle. The partons with the biggest radius are the light arm (LA) and the heavy arm (HA), they are involved first in a radial approach of two nucleons.

The masses and radii of the four partons of a nucleon carrying electroweak charges are listed in Table 1.

Table 1: Masses and radii of partons of nucleons bound in an alpha-particle

parton	mass - quantum	$m_{pt}c^2$ (MeV)	r_1 (fm)	r_2 (fm)
HA	m_8	122. 767	0.804	0.402
HL	m_8	245.258	0.402	0.201
LA	m_{41}	106.454	0.927	0.463
LL	m_{41}	213. 128	0.463	0.231

The attractive nuclear forces lead to a size of two bound nucleons from a legth $l_{\mathrm{mod}}(\alpha)$ (one side of a quadratic (2n2p) - structure)

$l_{\mathrm{mod}}(\alpha) \approx 4 * 0.804 = 3.216$ fm (calculated for the radii of the heavy arms) to

$l_{\mathrm{mod}}(\alpha) \approx 4 * 0.927 = 3.708$ fm (radii of the light arms).

These results have to be compared to the diameter calculated from the charge radius $r_{\mathrm{exp}}(\alpha)$ (rms) of the alpha-particle:

$2r_{\mathrm{exp}}(\alpha) = 2 * 1.6755\ fm = 3.351\ fm$, ([17])

The alpha-particle is seen as a spherical droplet in spacetime. The experimental value is within the attraction range of the model, with a smaller distance to the lower limit, determined by the heavy block. This represents a plausible relation.

The repulsion ranges from $2(0.804 + 0.402) = 2.412\ fm$ (assuming the radii of the heavy blocks are approaching) to $2(0.927 + 0.463) = 2.78\ fm$, (taking the radii of the light blocks).

These values correspond to an approach of the two nuclei down to the 'hard core' of both particles. The hard core is assumed to be determined by the contact of spin-parallel rotons, which have opposite tangential momenta at the

contact points as the origin of the repulsion. This corresponds to the 'cogwheel' picture, like the assumption of attractive forces by radial approach of rotons with anti-parallel spins.

However, the experimental hard core radii have the region 0.3 to 0.47 fm, leading to a distance of about 0.9 fm, if two particles could approach to the hard core - distance. The observed hard core is a factor of about three below the model estimation.

The radii of the internal rotons (r_2 - values) of 0.4 fm (HA) and 0.46 fm (LA) seem to correspond to the experimental hard core radii. Also an interaction of the legs (HL and LL) of the two nucleons in an alpha-particle could be taken into account. It is not clear, which of the 12 rotons of a nucleon - with 24 spatial dimensions on its 12 rotational planes - are actually involved in the repulsive action of the hard core.

The transition of the size of a nucleus in its eigenspace into an spatial extension in spacetime represents a rather complex problem, which cannot be solved in general in the current state of the model development.

4 Bosonic dineutrons, diprotons and (np) - pairs

4.1 Comparison of the separation energies of dineutron and diproton

The spin-compensated (bosonic) constituents of even - even nuclei can be divided in two categories: Dineutrons (n↑n↓) and diprotons (p↑p↓) on the on hand and (2n2p) = (n↑n↓p↑p↓) - groups on the other hand.

A dineutron or a diproton newly attached to a nucleus interacts with the whole reservoir of other constituents, already present in a nucleus (called 'distributed interaction'). In contrast, the (2n2p) groups like alpha-particles interact exclusively with the next neighbors within a nucleus (called 'contact interaction'). This will be discussed in the following for light nuclei.

In order to investigate different coupling variants separately, we consider spin-compensated dineutrons (2n) or diprotons (2p) alternatively attached to the same even - even reference nucleus with Z = N. Thus we compare the separation energies $S(n)$ and $S(p)$

$$S(n) = S(2n)/2; \qquad S(p) = S(2p)/2 \tag{20}$$

By this method we compare the mirror nuclei (Z,N+2) and (Z+2,N) with the reference nucleus (Z,N).

The separation energies of single protons and neutrons are included for comparison, however, this comparison is not very useful because of disturbing spin - orbit interactions in (Z,N+1) and (Z+1,N) nuclei with odd atomic masses A.

The result is shown in Fig. 11. The curves for (2n) or (2p) separation are very similar for mirror nuclei, despite its opposite slopes. The positive slope of the neutron - separation energy $S(n)$ is caused by the *increasing attraction* between the dineutron and the (np) - pairs in the reference nucleus. The decreasing curve

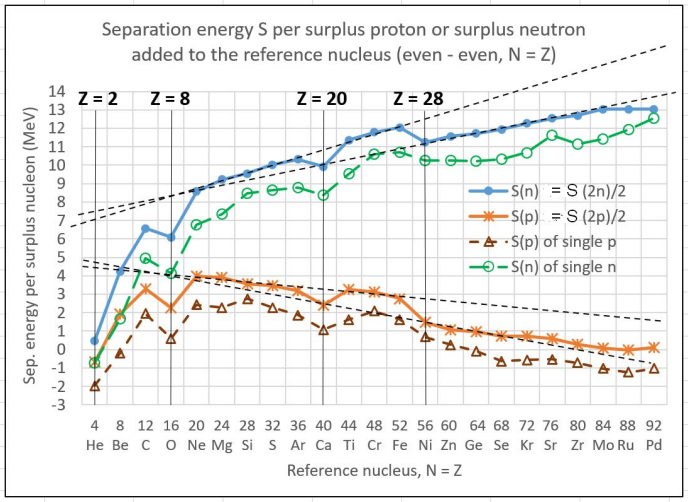


Figure 11: Comparison of the separation energies of protons and neutrons in mirror nuclei (Z, N + 2) and (Z + 2, N). The reference nuclei (Z, N) indicated on the abscissa are always even - even nuclei with atomic masses between A = 4 and 92.

of the proton separation energy $S(p)$ shows the *increasing repulsion* between the diproton and the (np) - pairs.

The increasing $S(n)$ and decreasing $S(p)$ trends can compensate each other, if a combined structure (2n2p) is formed. Thus (2n2p) - groups are spin - compensated (anti-parallel) as well as 'force - compensated'.

Two increasing and two decreasing dashed lines have crossing points at 16 O and describe regions of light nuclei ($20 \leq A < 56$) and of heavier nuclei ($56 \leq A < 86$). The slopes of the dashed lines in Fig. 11 are given in Table 2.

Table 2: Slopes of mirrored attraction and repulsion of dineutrons and diprotons

Interaction type	S (MeV)	$\Delta S/\Delta A$ (MeV/nucleon)	
	Start	Light nuclei	Heavy nuclei
	$A = 16$	$20 \leq A < 56$	$56 \leq A < 86$
$(nn) - (np)$ attraction	8.3	0.103	0.056
$(pp) - (np)$ repulsion	4.1	$-0,030$	-0.057

The attractive force is about a factor three stronger than the repulsion at light nuclei ($20 \leq A < 56$). However, attraction and repulsion are of equal strength at heavier nuclei (A > 56).

The consequences for nuclei with N = Z will be discussed in the following.

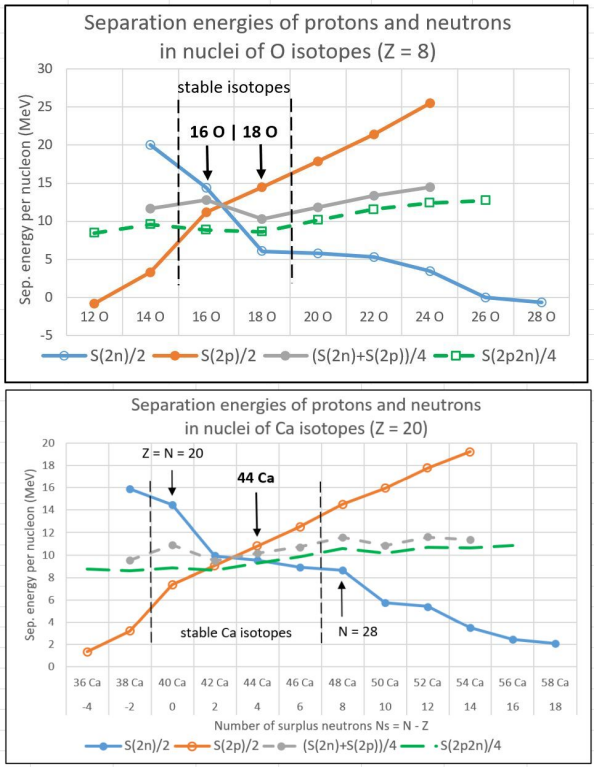


Figure 12: Comparison of separation energies of protons and neutrons in O- and Ca - isotopes. The attractive and repulsive effects of p and n compensate in (2n2p) - groups (e.g. alpha-particles) similar to an averaging of the effects.

4.1.1 The internal compensation of attraction and repulsion within a (2n2p) - group

The compensation of attractive and repulsive effects within a nucleus can be shown for different isotopic branches. We compare the separation energies $S(n)$ and $S(p)$ on the one hand, with their average and with the separation energy of S(2n2p)/4 on the other hand (see Figs. 12 and 13). The green dashed curves for S(2n2p)/4 show the compensation (similar to averaging, gray curves) of attractive and repulsive forces within a (2n2p) - group.

4.2 Several dineutrons attached to a nucleus

The separation energies per (2n2p) - group are nearly constant at light nuclei, indicating an interaction of an additional group with the next neighbors only. An increasing repulsion between an additional (2n2p) - group and the number of protons (already present in the nucleus) does not exist.

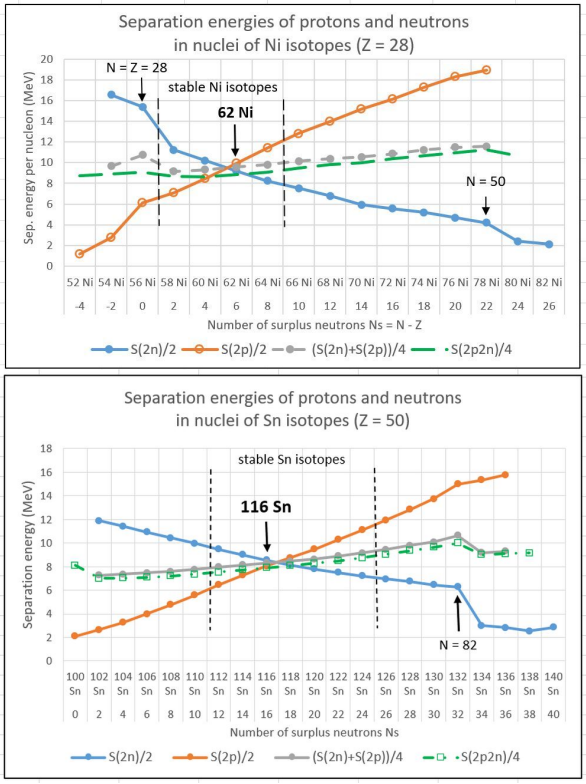


Figure 13: Comparison of separation energies of protons and neutrons in Ni- and Sn - isotopes. The attractive and repulsive effects of p and n compensate in (2n2p) - groups (e.g. alpha-particles) similar to an averaging of the effects.

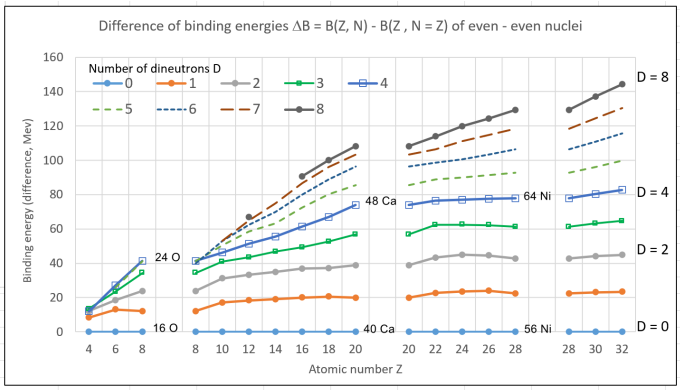


Figure 14: Increase of the binding energy by additional dineutrons for Z = 4 to 32. The role of the first four dineutrons starting at Z = 8 allows to assume a cross-like structure of the eigenspaces.

We investigate even - even nuclei along a selected path into the center of stability at Z = 50, see Fig. 15. We consider nuclei from 4 He to 116 Sn. Up to 40 Ca the nuclei with N = Z are stable, up to 56 Ni they are not really stable, but long-lived.

For atomic numbers Z > 20 all stable nuclei have one or more dineutrons.

Fig. 14 shows the gain of binding energy by adding D = 1 to 8 dineutrons in the region Z = 4 (Be) to Z = 32 (Ge). The first four dineutrons have for Z ≥ 8 nearly equidistant curves, its binding appears as equally favorably. They have four geometrically equivalent positions in the eigenspace with an energetically equal value. This indicates a symmetry with four directions of equal value. Therefore the eigenspaces are assumed to have a cross-like symmetry in one, two or three layers, see Figs. 23 and 24.

From Z = 30 (Zn) upwards, the (np) - (np) repulsion within the nucleus becomes stronger and additional dineutrons are necessary to compensate it. The path on the table of nuclides shows two steps of the attachment of 4 dineutrons, from 56 Ni to 64 Ni, and from 92 Mo to 100 Mo. The added dineutrons act as a 'shield' against the increasing (np) - (np) repulsion.

The N - Z - diagram can be divided into the two regions below and above Z = 50. Below the element Sn, the structure building is dominated by the force-compensated group (2n2p), realized as an alpha-particle or by two spin compensated entangeled (np) pairs.

The effect of aditional 'shielding' dineutrons added to N = Z nucleons from Z = 30 to 56 is shown in Fig. 16. The separation energy of a (np) - pair is as low as 15.5 MeV without dineutrons (D = 0), it increases to 16.8 MeV at D = 4 for Z = 30 to 42 and to about 19 MeV at D = 8, however only for Z = 30 to 34. Thus added dineutrons improve the binding of (np) - pairs.

The separation of the attraction between (nn) and (np) pairs and of the repulsion between (nn) pairs can be demonstrated separately with an example

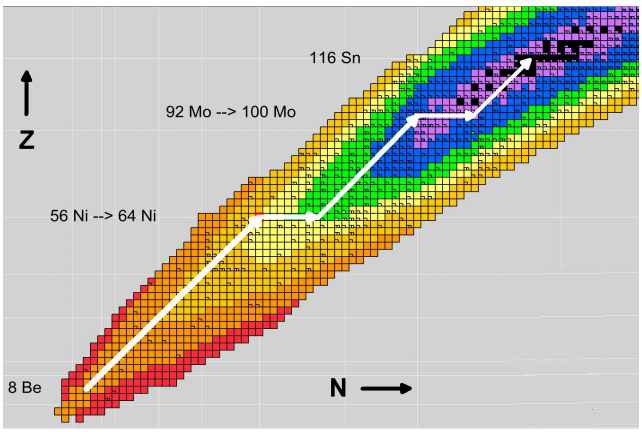


Figure 15: Path through the N - P-diagram of nuclides (white arrows) from Z = 4 to 50. Three intervals show $\Delta N = \Delta Z$, interrupted by two 'shielding' steps with $\Delta N = 8$, the addition of four dineutrons.

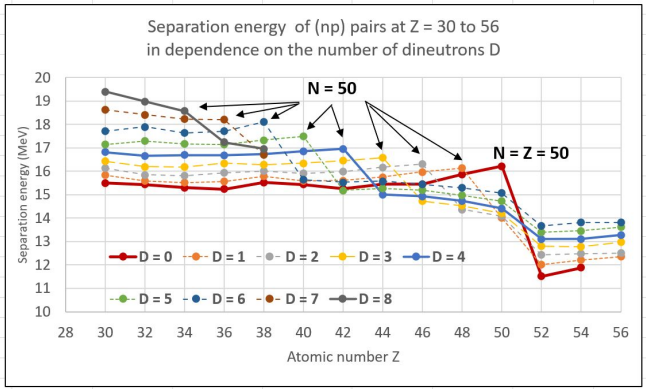


Figure 16: The effect of attached dineutrons at Z = 30 on the sparation energy of (np) pairs

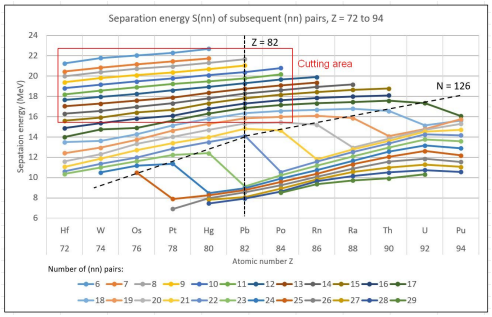


Figure 17: Separation energy of (nn) - pairs (dineutrons) between Z = 72 and 94. S(nn) forms a field of nearly parallel lines in the cutting area.

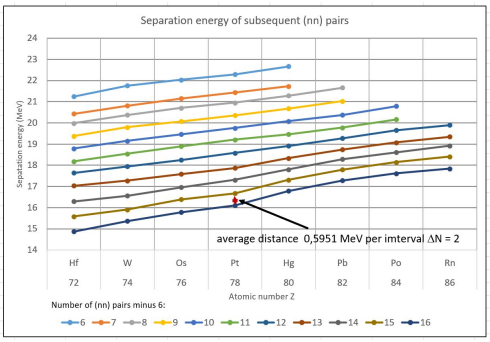


Figure 18: The separation energies of dineutrons in the cutting area show the combined effects of repulsion between dineutrons (along the isotopic branch of an element) and the attraction between dineutrons and (np) - groups (in different elemnts with increasing Z).

in the region Z > 72.

The separation energy of a dineutron at even - even nuclei is defined as $S(2n) = B(Z,N) - B(Z,N-2)$.

We use a cutting area, where the S(2n) - curves are nearly patallel lines, see Fig 17 and 18.

The separation energies per dineutron vary in two directions. The average differences between the even - even isotopes of an element ($\Delta N = 2$) vary from 0.679 MeV at Hf to 0.594 MeV at Ra. The overall average is 0.5951 MeV as shown in Fig. 18. Using this nearly constant factor, we transformed the curves into one line with a constant positive slope, see Fig. 19. This transformation neutralized the differences along the isotopic branch of each element, caused by (nn) - (nn) repulsion.

The resulting slope of 0.375 MeV per interval $\Delta Z = 2$ is caused by the increasing attraction between dineutrons and the increasing number of (2n2p)

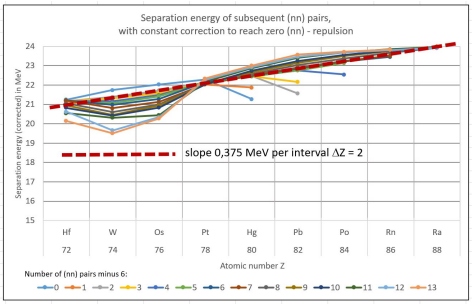


Figure 19: Correction of the repulsion between dineutrons by transformation of the curves into one curve of lightest isotope of each element.

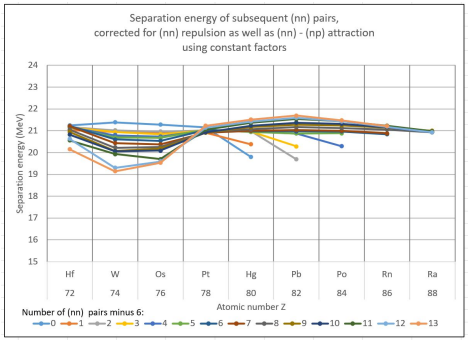


Figure 20: Correction of the attraction between dineutrons and (np) - groups by a trasformation of the line into a single value S(nn) at the level of Hf.

- groups in the nuclei from Hf to Ra. This effect can be neutralized in a second transformation.

The result approximates a horizontal line representing a nearly constant separation energy $S(2n) \approx 21MeV$, independent of (nn) - (nn) repulsion as well as of (nn) - (np) attraction (see Fig. 20).

A detailed knowledge of the strengths of repulsion and attraction would allow to determine the varying binding energy of a dineutron.

4.3 The local contact points

Two spin-compensated (np) - pairs are usually coupled to a (2n2p) - group within even - even nuclei. In space-time, such a group can be localizable in a nucleus as a 'preformed' alpha-particle or it can be non - localizable, but entangled and always spin-compensated. The (2n2p) - group represents the most stable structural component of nuclei. Each nucleon in a (2n2p) - group has internally two interaction partners. They interact like a ring of four nucleons, attracting each other.

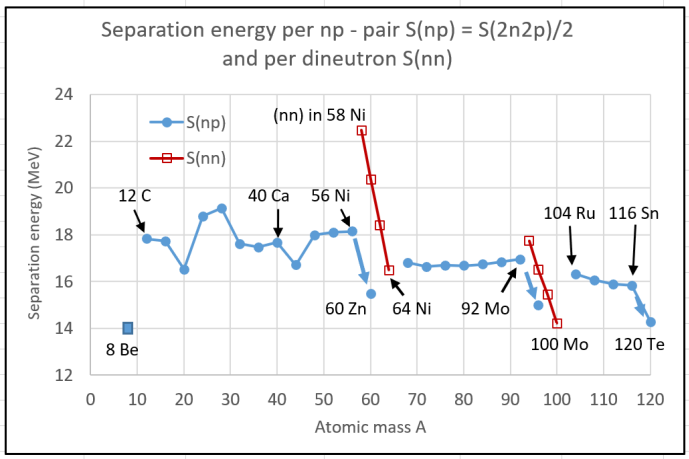


Figure 21: The separation energy of force-compensated (2n2p) groups is approximately constant for even-even nuclei with N = Z up to Z = 28. Further regions of constance appear for nuclei with N = Z + 8 (four 'shielding' dineutrons) between Z = 30 and Z = 46 and for nuclei with N = Z + 16 (8 shielding dineutrons) up to Z = 50.

We investigate the separation energies of (np) - groups
$S(np) = S(2n2p)/2$
for even - even nuclei, and we find Z - regions with nearly constant values of $S(np)$ (see Fig. 21, blue curves).

The separation energies of dineutrons S(nn) decrease sharply with the increasing number of dineutrons already present in the nucleus (see Fig. 21, red curves). This is caused by an increasing repulsion between dineutrons. In contrast, the separation energy S(np) is approximately constant (blue curves), in particular in the region Z = 6 to 28.

In classical electrostatics, an increasing repulsion would result from a collective Coulomb - field of an increasing number Z of protons. Therefore the separation energy S(np) should *decrease* with Z. However, empirically one finds essentially an independence of Z up to 56 Ni (Z = 28). Thus the Coulomb law is not applicable *within* a nucleus. This agrees with the basic - space models of proton and neutron. The integer electromagnetic charges in the models have only Coulomb *self*-interaction. An interaction *between* the em charges does not exist due to dimensional invisibility.

Conseqently, the total binding energy of even - even nuclei increases linearly with the number of (np) pairs up to Z = 28 for N = Z - nuclei. (see Fig. 22).

Nuclei containing four dineutrons such as 64 Ni show a linear behavior between Z = 28 and Z = 42 (up to 92 Mo). The additional four dineutrons compensate the increasing repulsion beween more than 28 protons. Nuclei containing eight dineutrons such as 100 Mo show an approximately linear increase

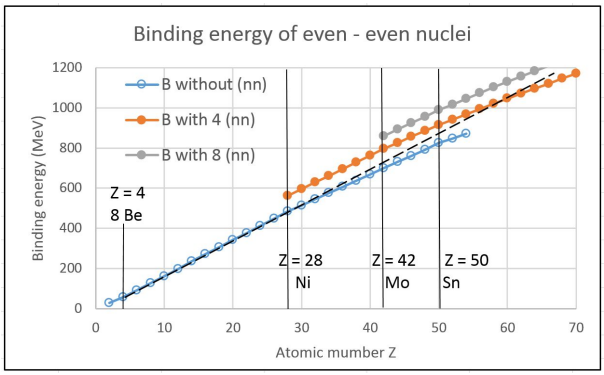


Figure 22: Three Z - regions have a linear increase of the binding energy with Z.

between Z = 42 and 50, up to 116 Sn.

4.4 The binding capacity of a dineutron, a diproton and an (np) - pair

The binding energies of dineutrons differ sharply within an isotopic branch (see the red curves in Fig. 21) and between different elements. The maximum value of the separation - energy of a dineutron amounts to 28.2089 MeV and has been measured for the first dineutron in Cadmium - nuclei, see Fig. **??**. One has to ask, whether this high separation energy can be attributed to the binding of one dineutron or it has to be explained by the interaction of more than two particles ('distant coupling').

The maximum binding capacity of one neutron is determined by the content of fluctuating charge pairs and by the possible change of the budget of charge clusters, that means the change from $m_4 = w_4^4 m_Q$ to $m_{41} = \frac{1}{2}(w_4^4+1)m_Q$ within the parton LA(light arm) due to the coupling. Such a skeleton - change has to be assumed in all cases, because the coupling of dineutrons with the fully symmetric (2n2p) - groups would require this kind of symmetrization. The contribution to the binding energy by a change in the skeleton of the parton LA (derived from the model of the free neutron, see Fig. 41) amounts to

$$B_{skel} = (32 + 28(b_4 - 1) + (w_8^2 + u_{16} - 2))(m_4 - m_{41}) = 1.996\,139\,5\ MeV$$

The loss of fluctuating charge pairs by one neutron during dress - coupling would contribute in maximum

$B_{light}(n) = (28(b_4-1))m_4 + (40(b_4-1)+14(b_4^2-1))m_{41} = 2.976\,715\ MeV$
from the partons of the light block and
$B_{heavy}(n) = (124(b_8 - 1) + 19(b_8^2 - 1))m_8 = 11.402\,489\ MeV$
from the partons of the heavy block of the neutron model.

The total binding capacity of a dineutron becomes

$$B(2n) \leq 2(B_{light}(n) + B_{heavy}(n) + B_{skel}) = 32.750\,687\ MeV \qquad (21)$$

This result allows to explain the maximum separation energy of a dineutron of 28.21 MeV exclusively by contact coupling, without assuming a contribution by distant coupling. The difference of around 4.5 MeV remains per dineutron, sufficient for the internal binding.

The maximum binding capacity of a proton is determined by the complete loss of fluctuating charges only, see Fig. 40:

The light block looses in maximum

$B_{light}(p) = (48(b_4 - 1) + 15(b_4^2 - 1))m_{41} \ = 2.406\,539\ MeV$
and the partons of the heavy block of the proton model can loose
$B_{heavy}(p) = (112(b_8 - 1) + 34(b_8^2 - 1))m_8 = 12.686\,253\ MeV$

The total binding capacity of a diproton becomes

$$B(2p) \leq 2(B_{light}(p) + B_{heavy}(p)) = 30.185\,584\ MeV \qquad (22)$$

The maximum value for a (np) - pair amounts to

$$B(np) \leq (B(2n) + B(2p))/2 = 31.468\,136\ MeV \qquad (23)$$

The separation energies of diprotons and (np) - pairs are always well below the maximum values of the corresponding binding energies. In general the origin of the binding energy of nuclei proposed in this article has no conflict with experimental data of even - even nuclei.

5 Nuclear eigenspaces

5.1 The geometry of nuclear eigenspaces of even - even nuclei with Z < 50

A (2n2p) - group consists of four nucleons as a ring-like structure without diagonal couplings. Two (2n2p) groups are connected like a ring of 4 (np) - groups. The nucleus 8 Be has nearly twice the binding energy of 4 He. That means, a nucleon has exact two binding partners in 8 Be, the same as in 4 He. Three (2n2p) - groups (12 C) and four such groups (16 O) have a somewhat higher binding energy per nucleon, caused by a certain content of nucleons with three binding partners. The binding energy of 12 C and 16 O is compatible with a geometry, where the (2n2p) - groups are connected at certain 'contact points', marked with two respective four red dots in Figure 23.

The three or four (2n2p) groups form a common eigenspace, and the (np) - groups not involved in this contact, are 'open ends' for the attachment of additional groups. However, the cross-like shape of the nuclear structure starting with 16 O may not be the energetic optimum in all cases. As an example, in the nucleus 20 Ne 5 (2n2p) - groups form of a pentagon, see Fig. 24. This

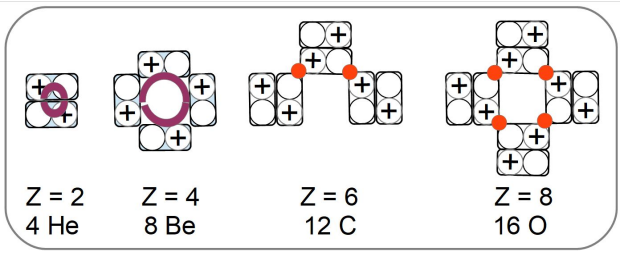


Figure 23: Eigenspaces of models of even - even nuclei as 2D - plots. At Z = 2 and 4 the models of the alpha-particle and the nucleus 8 Be show the ring-like coupling **within** the nuclei (violet color). At Z = 6 and 8 the contact coupling **between** different (2n2p) - groups is indicated (red points).

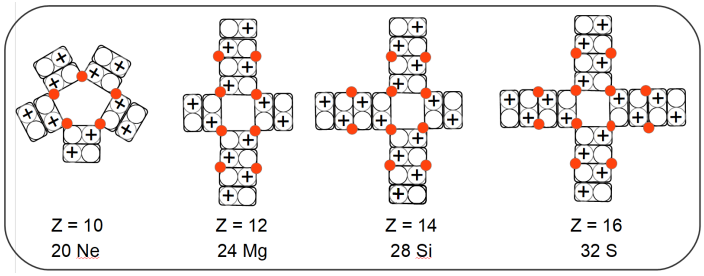


Figure 24: Eigenspaces of models of even - even nuclei at Z = 10 to 16 as 2D - plots. The number of contact points (red dots) is C = Z - 4, except for Z = 10, here one has C = Z/2 (pentagon - geometry).

assumption can be derived from the measured binding energies, see Table 4. The geometry of the light nuclei with N = Z = 2 to 28 results from a bottom - up process using the empirical values of the nuclei, in particular the binding energy [2]).

Axial coupling of nucleons may generate a coupling between nuclei belonging to different layers of the eigenspace. The differentiation into layers starts with Z = N = 20 (40 Ca). The approximate position of an axial coupling is marked in 2D plots by a dashed line (see Fig. 25 and 27).

The arrows in the figure indicate the points of connection of the two layers in the third dimension, vizualized in Fig. 26.

The separation energy of alpha-particles S(2n2p) depends on the overall symmetry of the nucleus. This influence within the group of even-even nuclei is small between 12 C and 56 Ni, however the differences are big in the group of odd-odd nuclei at $Z \prec 11$ (see Figs. 30, 31 and Table 5).

Table 3 shows the binding energies $B(np)_3$ of (np) - groups with three binding partners per nucleon. We selected six cross-symmetric nuclei, where N/2 = Z/2

[2] The nuclear data used in this article have the origin [3]

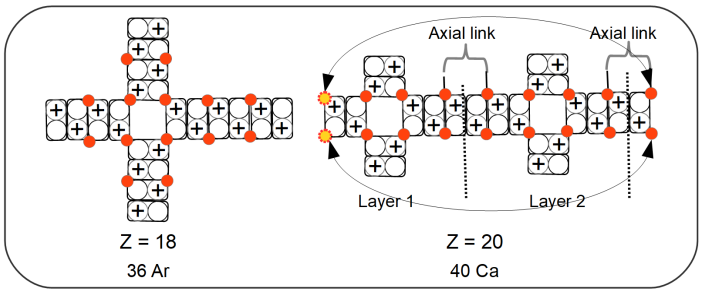


Figure 25: Eigenspaces of models of even - even nuclei as 2D - plots. The model of 36 Ar has C = Z - 4 = 14 and 40 Ca has Z - 4 = 16 contact points (red dots). The model of 40 Ca repeats the cross - like structure of 16 O at two layers, connected by two (2p2n) axial links between the layers.

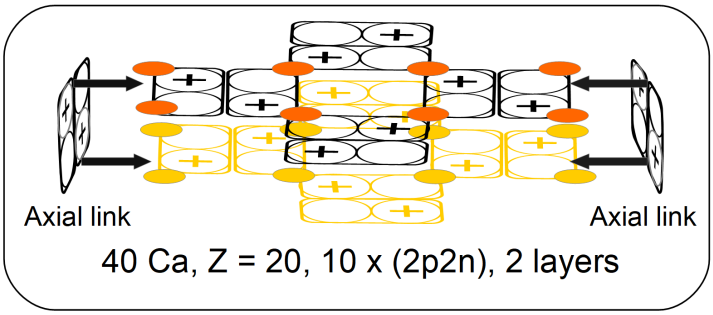


Figure 26: 3D - presentation of the eigenspace of 40 Ca. The cross - like structures of four (2n2p) - groups within each layer is realized by radial approach, between the two layers axial links exist (symbolically drawn at the left and the right side of the figure).

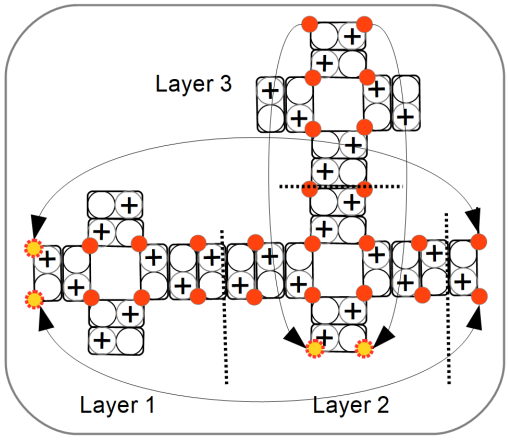


Figure 27: Eigenspace of the model of 56 Ni (Z = 28) with three layers as 2D - plot. The model has Z - 4 = 24 contact points.

Figure 28: Table 3: Binding energy $B(np)_3$ between three nucleons at cross - symmetric nuclei

Z = N	nuclide	B(np)_3 (MeV)		
		model	exp. (avg.)	mod. - exp.
8	16 O	17,765	17,757	0,008
12	24 Mg	17,765	17,708	0,057
16	32 S	17,765	17,932	-0,167
20	40 Ca	17,765	17,841	-0,076
24	48 Cr	17,765	17,744	0,021
28	56 Ni	17,765	17,809	-0,043

are even numbers.

we used two empirical values as model input for the calculation of $B(np)_{3,\mathrm{exp}}$ in Table 3:

$$B(np)_2 = B_\alpha/2 = 14.147832\ MeV \tag{24}$$

$$B(np)_3 = 17.765\ MeV \tag{25}$$

$B(np)_{3,\mathrm{mod}}$ approximates the value of the nucleus $B(16\ O)$. In the region Z = 6 to 28 the empirical values of $B(np)_{3,\mathrm{exp}}$ are approximately constant. Therefore one obtains a simple formula for the binding energy of light nuclei with N = Z:

Figure 29: Table 4: Binding energies of even - even nuclei at Z = 2 to 30 (B in MeV)

Z = N	nuclide	N(np)_2	N(np)_3	B_mod	B_exp	rel. dev.
2	4 He	2	0	28,2957	28,29566	**0,0000**
4	8 Be	4	0	56,5913	56,49949	0,0016
6	12 C	4	2	92,11987	92,16174	-0,0005
8	16 O	4	4	127,6484	127,61930	**0,0002**
10	20 Ne	5	5	159,5605	160,64480	-0,0067
12	24 Mg	4	8	198,7055	198,25702	0,0023
14	28 Si	4	10	234,2341	236,53683	-0,0097
16	32 S	4	12	269,7626	271,78013	-0,0074
18	36 Ar	4	14	305,2912	306,71672	-0,0046
20	40 Ca	4	16	340,8197	342,05212	-0,0036
22	44 Ti	4	18	376,3482	375,47488	0,0023
24	48 Cr	4	20	411,8768	411,46891	0,0010
26	52 Fe	4	22	447,4053	447,69785	-0,0007
28	56 Ni	4	24	482,9339	483,99562	-0,0022
30	60 Zn	4	26	518,4624	514,98300	0,0068

$$B(N, Z = N) \approx N(np)_2 * B(np)_2 + N(np)_3 * B(np)_3 \tag{26}$$

The values $N(np)_2$ and $N(np)_3$ are determined by the geometry of the eigenspaces and listed in Table 4. The binding energies $B(np)_2$ and $B(np)_3$ of the group (np) are the constants given in 24 and 25.

The relative deviations of B_{mod} from the experimetal values (besides 4 He and 16 O) are below one percent, see the last column in Table 4.

The difference between a three-partner and a two-partner coupling represents the average binding energy $B_{32,O}$ at a contact point of two (2n2p) - groups:

$$B_{32,O} = B(np)_3 - B(np)_2 = 3.60916\ MeV \tag{27}$$

The model representation of the contact point energy is approximately

$$B_{32,O} \approx 48(b_8 - 1)m_8 + 8(b_4 - 1)m_{41} = 3.617552\ \ MeV \tag{28}$$

Four components $(np)_2$ of the models in Table 4 indicate a structure with four 'open ends' of equal value, compatible with the assumption of a cross-like geometry of all nuclei with N = Z.

The additional loss of fluctuating charges by contact coupling, compared to the loss due to internal coupling within an alpha-particle, results in reduced average masses of proton and neutron, see Figs. 46 and 47 in the appendix. The contact point energy $B_{32,O}$ remains constant for Z $\leq$ 28. However, B_{32} decreases

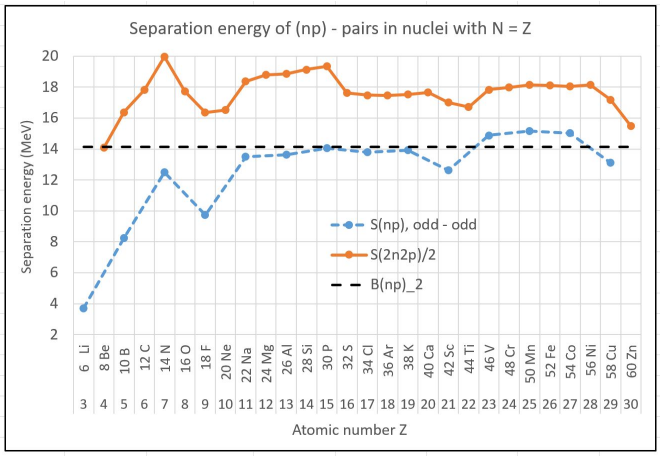


Figure 30: Separation energy per (np) - pair in even - even and in odd - odd nuclei.

for Z $>$ 28 due to an increasing repulsion between added (np) - groups and 28 (np) - groups already existing in the nucleus.

Thus $B(np)_3$ is not a constant independent of Z. In contrast, $B(np)_2$, half the energy of the *internal binding* within an (2n2p) - group, remains constant also for higher Z.

The model of the 'tunnel effect' The contact coupling between two (2n2p) - groups is not a static system. The contribution of any of the two groups to the contact energy B_{32} is equal in the average, however it may differ in a certain moment. This fluctuation of the contact energy between the contact partners may lead to the extreme case, that one group spends the full contact energy to 100 %, and the other to 0%. At such a rare moment, one of the (2n2p) - groups has the energy of a free alpha-particle and can leave the nucleus. This mechanism of alpha-decay is called 'tunnel effect' in quantum mechanics. Alpha-decay is common in super heavy nuclei with extremely small contact point energies. However, it may occur also in nuclei with medium atomic numbers like 104 Te (Z = 52), if the number of stabilizing dineutrons is zero or very low.

The picture of a 'tunnel' through a potential wall is used in spacetime, but not appropriate in basic space.

Models of odd - odd nuclei Odd - odd nuclei have a separation energy of the 'last' (np) - group nearly equal to $B(np)_2$, see Fig. 30. This indicates, that additional contact points do not emerge caused by the last (np) - group.

Assuming five 'open ends' instead of four in the eigenspace, the average values of $(np)_{3,\mathrm{exp}}$ for odd-odd nuclei In the region Z = 11 to 29 are equal to the values for even - even nuclei, where four 'open ends' exist (see Fig. 31).

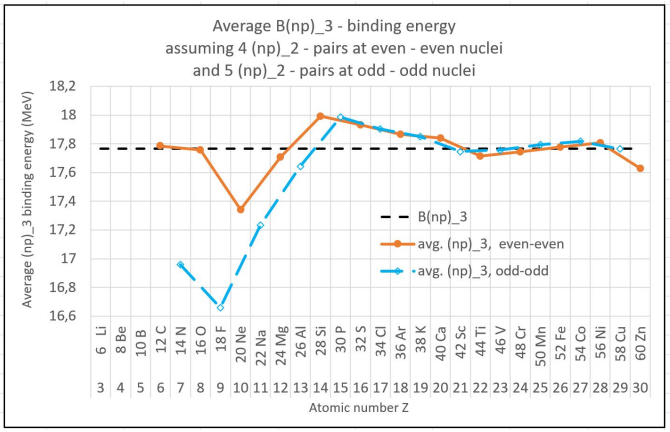


Figure 31: Binding energy $B(np)_3$ at Z = 6 to 30. Comparison of even - even nuclei (assumming C = Z - 4 contact points) and odd - odd nuclei (assuming C = Z - 5 contact points).

The light odd - odd nuclei can be modelled using the models of an even - even nucleus and adding a (np) group at one side of an arm like a parasite. This geometry allows to calculate the binding energy assuming five instead of four $(np)_2$ groups.

Table 5 shows the results. The geometric model requires an arm of sufficient length, see Fig. 32. The calculation of the binding energy was performed using formula **??**.

The geometric picture of odd - odd nuclei seems to be applicable for Z = N $\geq$ 13 (26 Al). The calculated binding energies agree well with the experimental values. In contrast, the lightest odd - odd nuclei 6 Li and 10 B cannot be modelled by this method, see Table 5.

5.2 The structure of heavy even - even nuclei with Z > 50

At Z = 50, the nuclear structure changes due to a change in the internal force-compensation of the attracting and repulsing interactions between nucleons. This change can be seen by comparison of the separation energy of (2n2p) for Z > 50 with that in the region Z < 50. The sharp decrease at Z = 52 and Z = 84 is shown, however, detailed geometric information is difficult to extract (see Fig. 34).

While up to Z = 50 essentally the group (2n2p) dominates (with stepwise (2n) complements), in the region Z > 50 a higher contribution of (2n) is required for internal compensation. Approximately each (2n2p) is combined with a dineutron (2n) in order to achieve (4n2p) groups with an internal compensation of attractive and repulsive forces.

From 112 Sn to 208 Pb the difference of the number of protons is

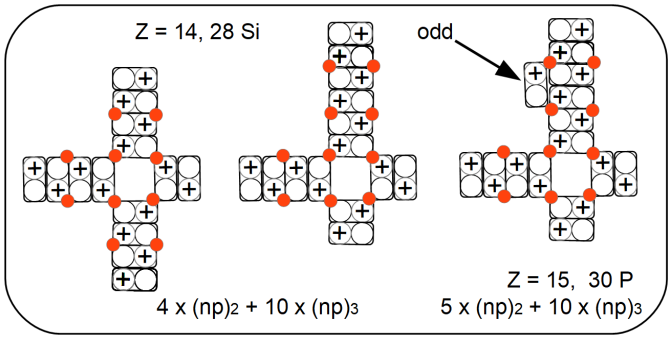


Figure 32: 2D - plots of eigenspaces of 28 Si and 30 P. Both nuclei have identical numbers of contact points. The odd - odd nucleus 30 P has 5 instead of 4 $(np)_2$-pairs.

Figure 33: Table 5: Binding energies of odd - odd nuclei at Z = 3 to 29 (B in MeV)

Z = N	nuclide	N(np)_2	N(np)_3	B_mod	B_exp	rel. dev.
3	6 Li	3	0	42,4429	31,99399	**0,3266**
5	10 B	5	0	70,73816	64,75083	**0,0925**
7	14 N	5	2	106,2687	104,65861	0,0154
9	18 F	5	4	141,7993	137,36948	0,0322
11	22 Na	5	6	177,3298	174,14456	0,0183
13	26 Al	5	8	212,8603	211,89389	0,0046
15	30 P	5	10	248,3909	250,60518	-0,0088
17	34 Cl	5	12	283,9214	285,56501	-0,0058
19	38 K	5	14	319,452	320,64624	-0,0037
21	42 Sc	5	16	354,9825	354,68706	0,0008
23	46 V	5	18	390,5131	390,36253	0,0004
25	50 Mn	5	20	426,0436	426,63410	-0,0014
27	54 Co	5	22	461,5742	462,73788	-0,0025
29	58 Cu	5	24	497,1047	497,11626	0,0000

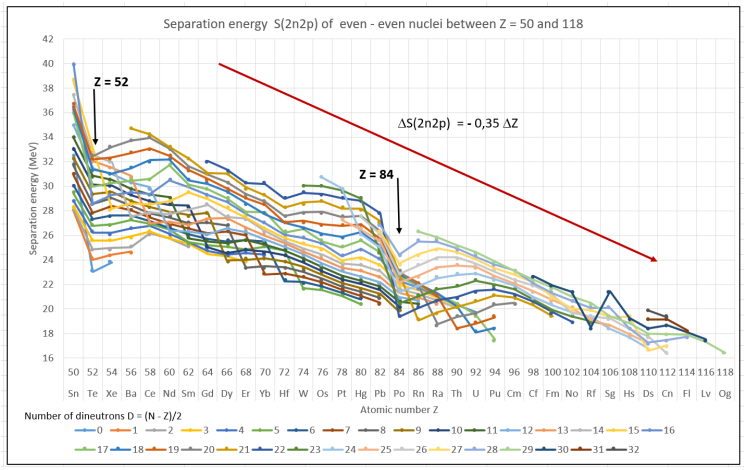


Figure 34: The separation energy S(2n2p) shows a general decrease with increasing Z..The slope is $\Delta S(2n2p) \approx -0.35 \Delta Z.AtZ$. At Z = 52 and Z = 84 has the separation energy significant lower values because the binding of (2n2p) on the magic structures at Z = 50 and Z = 82 is poor.

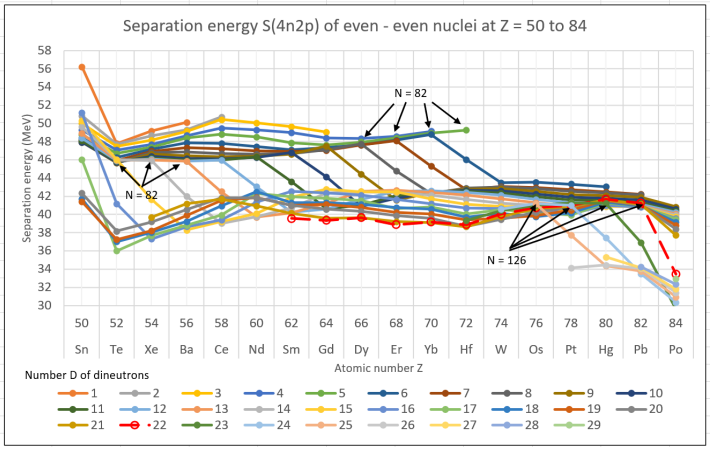


Figure 35: The separation energies of the group (4n2p) at even - even nuclei with Z = 50 to 84 is shown. S(4n2p) corresponds to the loss of an alpha-particle plus a dineutron. A stepwise transition between two geometries with different binding strengths is displayed. The transition starts from a higher level (46 to 48 MeV) and goes to a lower level (39 to 42 MeV),

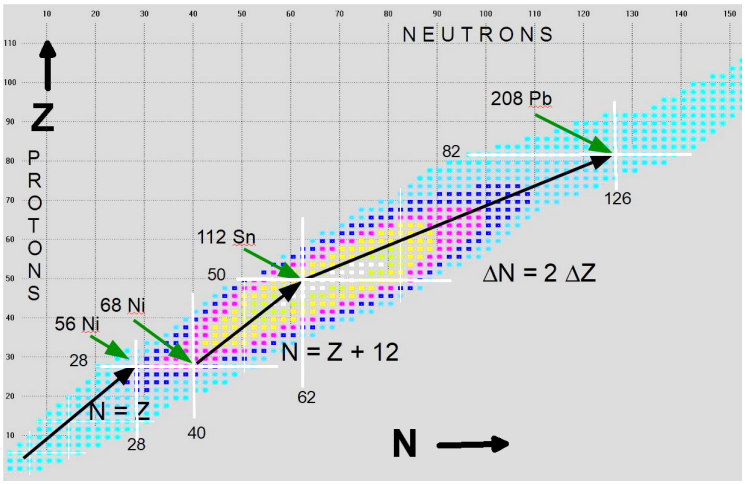


Figure 36: Two slopes exist along the path through the N - Z diagram. The light nuclei up to Z = 50 have the slope $\Delta N = \Delta Z$. The group (2n2p) dominates. The heavy nuclei with Z > 50 have the slope $\Delta N = 2\Delta Z$.The group (4n2p) replaces (2n2p).

$\Delta Z = 82 - 50 = 32$, and the difference of the number of neutrons amounts to

$\Delta N = 126 - 62 = 64$. The relation is $\Delta N = 2\Delta Z$.

208 Pb and 112 Sn are used as the reference nuclei in the high Z region and in the valley of stability, respectively.

The relation $\Delta N = 2\Delta Z$ indicates, that a new force-compensated group is in action, that is (4n2p), see Fig. 36.

The difference of binding energies of even – even nuclei with $\Delta N = 2\Delta Z$ - equal to the separation energies of (4n2p) - are approximately constant, there is no deccrease with increasing Z. The separation energy S(4n2p) does not depend on the number of protons or neutrons already present in the nucleus. This is true within certain limits, for instance for the regions between Z = 52 (Te) and Z = 60 (Nd) as well as between Z = 62 (Sm) and Z = 82 (Pb), see the examples in Fig. 37. 16 structural steps, each (4n2p) wide, are needed to cross the 'valley of stability', e.g. from 112 Sn to 208 Pb. The separation energy per step is approximately 46 MeV for the first 5 steps and 41 MeV for the remaing 10 steps..

The separation energy remains constant in wide intervals of Z. The group (4n2p) has an internal compensation of attracting and repulsing forces. (4n2p) at Z > 50 seems to play a similar role like (2n2p) at Z $\leq$ 50.

Above the element Pb, the group (4n2p) is not able to compensate all forces internally. The picture of the separation energies at different numbers of dineutrons appear disturbing (see Fig. 38). However, the curves of the separation energies S(6n2p) look disentangled (see Fig. 39).

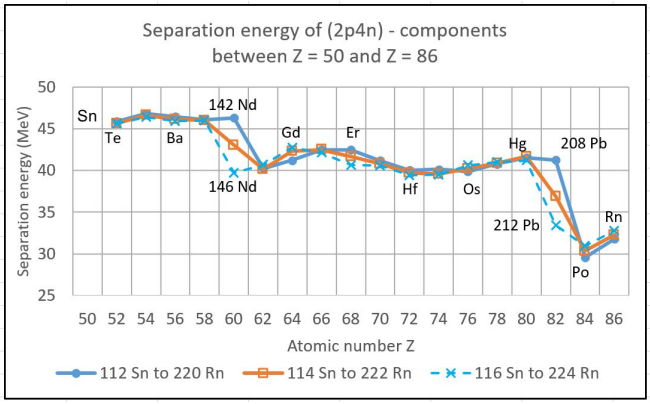


Figure 37: The separation energy for the (4n2p) - group is approximately constant in the regions Z = 50 to 58 and Z = 60 to 82.

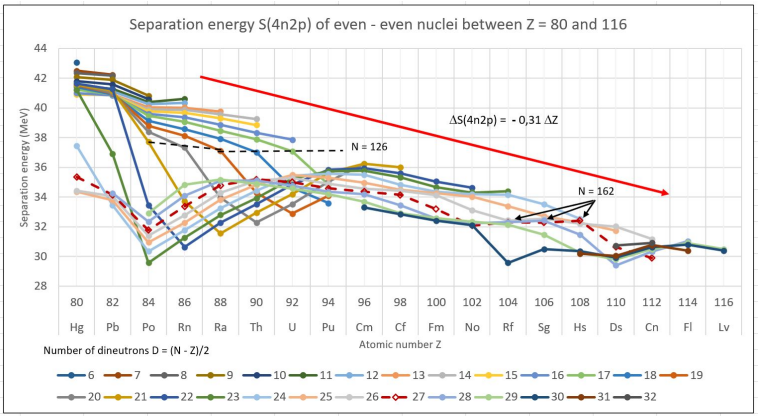


Figure 38: Separation energy S(4n2p) in the region Z > 82. The dependence of the energies on the number of dineutrons provides a somewhat confusing picture.

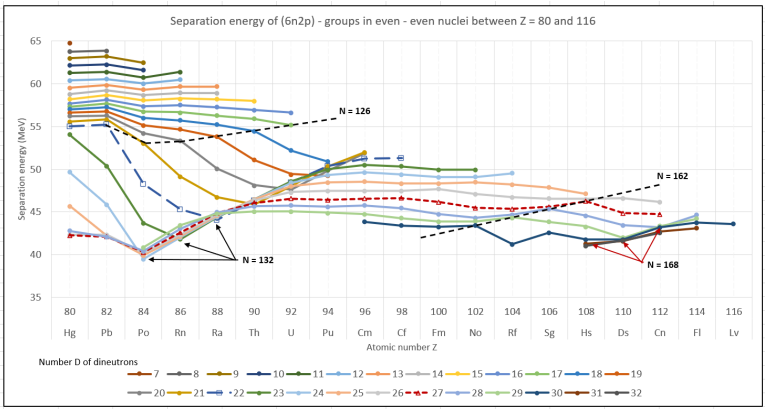


Figure 39: Separation energy S(6n2p) for Z > 82. The combination of each (2n2p) with *two* additional dineutrons provides an undisturbed picure of nearly horizontal lines. The changes between different geometries of the eigenspaces above N = 126 and N = 162 are clearly visible.

The combination of one (2n2p) and 2(nn) seems to be the characteristics of force-compensation in nuclei above the element Pb (Z = 82).

6 Conclusions

The structure and the binding energy of the deuteron, the alpha-particle and light nuclei can be modelled in an extra space called 'basic space', not embedded in spacetime.

Nuclear coupling between two originally separated nucleons can be understood as formation of a common eigenspace of the nucleons. This requires a smaller quantity of fluctuating charge pairs. The energy of the disappearing charge pairs represents the binding energy, by reducing the total mass of the system of the bound nucleons.

This concept has been tested using even – even and partly also odd – odd nuclei. Only spin-compensated, bosonic components of nuclei such as (2n2p) – groups, dineutrons, diprotons and (np) – pairs have been considered. The Pauli exclusion principle has not to be observed during the model construction. The model is adjusted using empirical data of the ground states of 4 He and 16 O nuclei, the adjustment parameters have a quantitative model representation.

The resulting binding energies show an agreement between model – values and observed data within a deviation of 1 % in the region Z <= 28.
The (2n2p) – group within a nucleus shows an internal compensation of attracting and repulsing forces, which enables a constant contact energy between two (2n2p) – groups. The contact energy becomes part of the binding energy of the nucleus.

The contact energy is a constant in the region Z <= 28, independent of the

number of protons already present in the nucleus. This excludes the existence of a collective Coulomb – field in the common eigenspace of the bound nucleons. Such a non-classical behavior of light nuclei appears as the natural consequence of the models of baryons described in [13]. In these models, the partons of a neutron carry two integer electromagnetic (em) charges, the partons of a proton carry three em charges. The force-free rotating em – charges have Coulomb self-interaction along its circular path, however no Coulomb interaction between them.

In addition to the loss of fluctuating charges by 'dress coupling', also a change of the *skeleton* of the neutron plays a role in the nuclear coupling. Bound nucleons tend to synchronize their components, such that the partons achieve identical frequencies by adaptation of their rotating masses. The neutron is forced to reduce its mass to achieve the lower parton masses of the proton. The effect of synchronization results in absolutely identical skeleton masses of proton and neutron bound in a nucleus. The consequence for the neutron is to achieve the same stability as the proton, in contrast to the unstable free neutron.

7 Appendix

7.1 Energy factors of circulating charges as function of $z = \alpha/\pi$

$z = 2.322\,819\,465 \times 10^{-3}$

$b_k = 1 + kz$; example $b_4 = 1.009\,291\,278$

$d_k = 1 + kz + (kz)^2$

$a_k = 1 + kz + (kz)^2 + (kz)^3$

$w_k = 1 + kz + (kz)^2 + (kz)^3 + ... = \frac{1}{1-kz}$; example $w_4 = 1.009\,378\,415\,3$

$u_k = 1 - kz - (kz)^2 + (kz)^3 + (kz)^4 - (kz)^5 - (kz)^6 + (kz)^7 + (kz)^8 - (kz)^9 - (kz)^{10} + (kz)^{11} + (kz)^{12}$

7.2 Models of free and bound nucleons

This section contains formal expressions for masses and relative magnetic moments of the models of proton and neutron in its free state and as components of the deuteron and the alpha-particle. Models of proton and neutron in two or more (2n2p) - groups, bound by contact points, are also given.

Parton	Proton (free): Parton mass formula	p Mass, MeV
ear 1	$32b_8m_8$	123. 191 264
ear 2	$32b_8m_8$	123. 191 264
HA ⊖	$(32+16(b_8^2-1)+6(b_8-1)+(2w_8+2w_{16}+u_{32}-5))m_8$	123. 768 288
HL	$(64+18(b_8^2-1)+42(b_8-1)+(2w_{16}+u_{32}-3))m_8$	247. 380 899
LA ⊕	$(32+4(b_4^2-1)+16(b_4-1)+(2w_4+2w_8+u_{16}-5))m_{41}$	106. 871 624
LL ⊕	$(64+11(b_4^2-1)+32(b_4-1)+(2w_4+2w_8+u_{16}-5))m_{41}$	213. 868 790
proton	exp.: m_p = 938. 272 088 MeV	938. 272 129

Parton	p (free): Parton μ/μ_N calculation	p μ/μ_N(mod)
HA ⊖	$-m_p/(2*123.768288)$	− 3. 790 438 18
LA ⊕	$+m_p/(2*106.871624)$	4. 389 715 68
LL ⊕	$+m_p/(2*213.868790)$	2. 193 569 45
proton	μ/μ_N(exp) = 2. 792 847 34	2. 792 846 96

Figure 40: Model of the free proton

Parton	Neutron (free): Parton mass formula	Mass, MeV
ear 1	$32b_8m_8$	123. 191 264
ear 2	$32b_8m_8$	123. 191 264
HA ⊖	$(32+24(b_8-1)+2(b_8^2-1)+(2w_8+2w_{16}+u_{32}-5))m_8$	123. 047 690
HL ⊕	$(64+36(b_8-1)+17(b_8^2-1)+(2w_8+w_{16}^2+u_{32}-4))m_8$	246. 966 488
LA	$(32+28(b_4-1)+(w_8^2+u_{16}-2))m_4$	108. 928 825
LL	$(64+40(b_4-1)+14(b_4^2-1)+(w_8^2+u_{16}-2))m_{41}$	214. 239 836
neutron	exp. m_n = 939. 565 421 MeV	939. 565 367

Parton	n (free): Parton μ/μ_N calculation	μ/μ_N(mod)
HA ⊖	$-m_p/(2*123.04769)$	− 3. 812 635 9
HL ⊕	$+m_p/(2*246.966488)$	+ 1. 899 593 9
neutron	μ/μ_N(exp) = − 1. 913 042 7	−1. 913 042

Figure 41: Model of the free neutron

Parton	Proton in deuteron: Parton mass formula, HA reduced	p Mass, MeV
ear 1	$32b_8m_8$	123. 191 265
ear 2	$32b_8m_8$	123. 191 265
HA ⊖	$(32+28(b_8-1)+(2w_8+2w_{16}+u_{32}-5))m_8 = 123.\,045\,079\,33$	123. 045 079
HL	$(64+18(b_8^2-1)+42(b_8-1)+(2w_{16}+u_{32}-3))m_8 = 247.\,380\,898\,67$	247. 380 899
LA ⊕	$(32+4(b_4^2-1)+16(b_4-1)+(2w_4+2w_8+u_{16}-5))m_{41} = 106.\,871\,623\,67$	106. 871 624
LL ⊕	$(64+11(b_4^2-1)+32(b_4-1)+(2w_4+2w_8+u_{16}-5))m_{41} = 213.\,868\,789\,91$	213. 868 790
p in d	total mass	937. 548 922

Parton	Parton μ/μ_N calculation	p in d μ/μ_N(mod)
HA ⊖	$-m_p/(2*123.\,045\,079)$	− 3. 812 716 8
LA ⊕	$+m_p/(2*106.\,871\,624)$	4. 389 715 7
LL ⊕	$+m_p/(2*213.\,868\,790)$	2. 193 569 5
p in d	μ/μ_N	2. 770 568 3

Figure 42: Model of the proton bound in a deuteron

Parton	Neutron in deuteron: Parton mass formula, reduced HA, LA, LL	Mass, MeV
ear 1	$32b_8m_8$	123. 191 264
ear 2	$32b_8m_8$	123. 191 264
HA ⊖	$(32+28(b_8-1)+(2w_8+2w_{16}+u_{32}-5))m_8 = 123.\,045\,079\,33$	123. 045 079
HL ⊕	$(64+36(b_8-1)+17(b_8^2-1)+(2w_8+w_{16}^2+u_{32}-4))m_8 = 246.\,966\,488$	246. 966 488
LA	$(32+16(b_4^2-1)+12(b_4-1)+(w_8^2+u_{16}-2))m_{41} = 107.\,430\,032\,87$	107. 430 033
LL	$(64+40(b_4-1)+14(b_4^2-1)+(w_8^2+u_{16}-2))m_{41} = 214.\,239\,835\,51$	214. 239 836
n in d	total mass	938. 063 965

Parton	Parton μ/μ_N calculation	μ/μ_N(mod)
HA ⊖	$-m_p/(2*123.\,045\,079) = -3.\,812\,716\,834\,5$	− 3. 812 716 8
HL ⊕	$+m_p/(2*246.\,966\,488) = 1.\,899\,593\,940\,5$	+ 1. 899 593 9
n in d	μ/μ_N	−1. 913 042

Figure 43: Model of the neutron bound in a deuteron

Parton	Proton in alpha-particle, parton mass formulas	Mass, MeV
ear 1	$(32+16(b_8-1))m_8$	122. 067 549
ear 2	$(32+16(b_8-1))m_8$	122. 067 549
HA ⊖	$(32+2(b_8^2-1)+20(b_8-1)+(2w_8+2w_{16}+u_{32}-5))m_8$	122. 766 759
HL	$(64+4(b_8^2-1)+38(b_8-1)+(w_{16}^2+u_{32}-2))m_8$	245. 120 813
LA ⊕	$(32+4(b_4^2-1)+8(b_4-1)+(2w_4+2w_8+u_{16}-5))m_{41}$	106. 625 239
LL ⊕	$(64+4(b_4^2-1)+24(b_4-1)+(2w_4+2w_8+u_{16}-5))m_{41}$	213. 189 230
p in α	total mass	931. 837 125

Figure 44: Model of the proton, bound in an alpha-particle

Parton	Neutron in alpha-particle, parton mass formulas	Mass, MeV
ear 1	$(32 + 16(b_8 - 1))m_8$	122. 067 542
ear 2	$(32 + 16(b_8 - 1))m_8$	122. 067 542
HA ⊖	$(32 + 2(b_8^2 - 1) + 20(b_8 - 1) + (2w_8 + 2w_{16} + u_{32} - 5))m_8$	122. 766 759
HL ⊕	$(64 + 4(b_8^2 - 1) + 38(b_8 - 1) + (2w_8 + 2w_{16} + u_{32} - 5))m_8$	245. 258 307
LA	$(32 + 4(b_4^2 - 1) + 8(b_4 - 1) + (w_8^2 + u_{16} - 2))m_{41}$	106. 564 254
LL	$(64 + 4(b_4^2 - 1) + 24(b_4 - 1) + (w_8^2 + u_{16} - 2))m_{41}$	213. 128 245
n in α	total mass	931. 852 648

Figure 45: Model of the neutron, bound in an alpha-particle

Parton	Proton in $(np)_3$ of 16 O, parton mass formulas	Mass, MeV
ear 1	$(32 + 16(b_8 - 1))m_8$	122. 067 549
ear 2	$(32 + 16(b_8 - 1))m_8$	122. 067 549
HA ⊖	$(32 + 2(b_8^2 - 1) + 12(b_8 - 1) + (2w_8 + 2w_{16} + u_{32} - 5))m_8$	122. 204 898
HL	$(64 + 4(b_8^2 - 1) + 22(b_8 - 1) + (w_{16}^2 + u_{32} - 2))m_8$	243. 997 091
LA ⊕	$(32 + 4(b_4^2 - 1) + 8(b_4 - 1) + (2w_4 + 2w_8 + u_{16} - 5))m_{41}$	106. 625 239
LL ⊕	$(64 + 4(b_4^2 - 1) + 20(b_4 - 1) + (2w_4 + 2w_8 + u_{16} - 5))m_{41}$	213. 066 038
p in $(np)_3$	total mass	930. 028 364

Figure 46: Model of the proton bound in a light nucleus as part of $m(np)_3$

Parton	Neutron in $(np)_3$ of 16 O, parton mass formulas	Mass, MeV
ear 1	$(32 + 16(b_8 - 1))m_8$	122. 067 542
ear 2	$(32 + 16(b_8 - 1))m_8$	122. 067 542
HA ⊖	$(32 + 2(b_8^2 - 1) + 12(b_8 - 1) + (2w_8 + 2w_{16} + u_{32} - 5))m_8$	122. 204 898
HL ⊕	$(64 + 4(b_8^2 - 1) + 22(b_8 - 1) + (2w_8 + 2w_{16} + u_{32} - 5))m_8$	244. 134 584
LA	$(32 + 4(b_4^2 - 1) + 8(b_4 - 1) + (w_8^2 + u_{16} - 2))m_{41}$	106. 564 254
LL	$(64 + 4(b_4^2 - 1) + 20(b_4 - 1) + (w_8^2 + u_{16} - 2))m_{41}$	213. 005 052
n in $(np)_3$	total mass	930. 043 872

Figure 47: Model of the neutron bound in a light nucleus as part of $m(np)_3$

References

[1] Yukawa H. (1935): On the interaction of elementary particles I. In: Proceedings of the Physico-Mathematical Society of Japan. 3. Series, Vol. 17, 1935, p. 48–57

[2] Weise W. (2206), Yukawa's Pion, Low-Energy QCD and Nuclear Chiral Dynamics, Yukawa - Tomonaga Centennial Symposium, Kyoto Dec. 13 (2006)

[3] The AME 2020 atomic mass evaluation (II). Tables, graphs and references, Meng Wang et al 2021 Chinese Phys. C 45 030003

[4] Schaeffer B., Pairing Effect on the Binding Energy Curve of N = Z Atomic Nuclei, World Journal of Nuclear Science and Technology, 2013, 3, 79-82; http://dx.doi.org/10.4236/wjnst.2013.33013; Published Online July 2013 (http://www.scirp.org/journal/wjnst)

[5] Oertzen W. von, M. Freer and Y. Kanada-En'yo, (2006) Nuclear clusters and nuclear molecules, Physics Reports, Vol. 432, No. 2, 2006, pp. 43-113. doi:10.1016/j.physrep.2006.07.001

[6] Freer M., Hisashi Horiuchi, Yoshiko Kanada-En'yo, Dean Lee, Ulf-G. Meißner, Microscopic Clustering in Light Nuclei, Rev. Mod. Phys. 90, 035004 (2018), doi 10.1103/RevModPhys.90.035004

[7] Coraggio L., A. Covello et al. From Kuo-Brown to today's realistic shell-model calculations, Nucl. Phys. A 928 (2014) 43, doi: https://doi.org/10.1016/j.nuclphysa.2014.03.018

[8] Povh B., Rith K et al., Teilchen und Kerne, Eine Einführung in die physikalischen Konzepte, Springer 2014, ISBN 978- 3-642- 37821-8, doi 10.1007/ 978-3- 642- 37822-5

[9] Pfeifer W. An Introduction to the Interacting Boson Model of the Atomic Nucleus (PDF, 1998). ISBN 978-3-7281-2520-0

[10] Arima, A; Iachello, F (1981). "The Interacting Boson Model". Annual Review of Nuclear and Particle Science. Annual Reviews. 31 (1): 75–105. doi:10.1146/annurev.ns.31.120181.000451. ISSN 0163-8998

[11] Herrmann H.-D. (2025), A joint Model of Particles and Spacetime, https://philarchive.org/rec/HERAJM-2

[12] Herrmann H.-D. (2026), Mass Quantization and the Upper Limit of Particle Mass, https://philarchive.org/rec/HERMQA-2

[13] Herrmann H.-D. (2026), Baryon models in a circular extra space, https://philarchive.org/rec/HERBMI-2

[14] CODATA Internationally recommended 2022 values of the Fundamental Physical Constants https://physics.nist.gov/cuu/Constants/index.html, retrieved March 2026

[15] Skyrme T.H.R., (1959) The effective nuclear potential, Nuclear Physics, volume 9, pages 615–634 (1959).

[16] Nomura, K. (2025) Mapped interacting boson model for nuclear structure studies. Eur. Phys. J. A 61, 139 (2025). https://doi.org/10.1140/epja/s10050-025-01604-7

[17] Angeli I., K.P. Marinova (2013), Table of experimental nuclear ground state charge radii: An update, Atomic Data and Nuclear Data Tables, IAEA, Nuclear data services, https://www-nds.iaea.org/radii/, retrieved Oct. 2026